Published in final edited form as:
Cell. 2010 May 14; 141(4): 656–667. doi:10.1016/j.cell.2010.04.009.

Mitochondria supply membranes for autophagosome biogenesis during starvation

Dale W. Hailey, **Peter K. Kim**, **Prasanna Satpute-Krishnan**, **Angelika S. Rambold**, **Kasturi Mitra**, **Rachid Sougrat**, and **Jennifer Lippincott-Schwartz**
National Institutes of Health, National Institutes of Child Health and Human Development, Cell Biology and Metabolism Program

Abstract

Starvation-induced autophagosomes engulf cytosol and/or organelles and deliver them to lysosomes for degradation, thereby re-supplying depleted nutrients. Despite advances in understanding the molecular basis of this process, the membrane origin of autophagosomes remains unclear. Here, we demonstrate that, in starved cells, autophagosomes are derived from the outer membranes of mitochondria. In time-lapse movies, the early autophagosomal marker, mApg5, transiently localizes to punctae on the surface of mitochondria, followed by the late autophagosomal marker, LC3. A unique tail-anchored outer mitochondrial membrane protein, but not other outer nor inner mitochondrial membrane proteins, labels autophagosomes and diffuses into newly forming autophagosomes from mitochondria. The fluorescent lipid, NBD-PS (which converts to PE in mitochondria) transfers from mitochondria to autophagosomes in starved cells. In addition, when mitochondria/ER connections are perturbed by loss of mitofusin2, starvation-induced autophagosomes do not form. Mitochondria thus play a central role in starvation-induced autophagy, serving as membrane source of autophagosomes.

INTRODUCTION

During starvation, many organisms retrieve molecules and energy via bulk degradation of their own intracellular components. This process has been termed macroautophagy, or simply autophagy—“self eating”. The execution of autophagy involves formation of multilamellar organelles that engulf cytosolic contents including proteins, protein aggregates, and entire organelles *en masse*. Lysosomes subsequently fuse with autophagosomes, delivering lysosomal proteases that degrade captured substrates within this hybrid structure, called an autolysosome. Transporters and permeases within the membrane of the autolysosome then move components released by catabolism back to the intracellular environment (Xie and Klionsky, 2007).

The requirement for autophagy during starvation has been demonstrated across the eukaryotic domain. In the absence of functional autophagy, *S. cerevisiae* cells die more readily when cells are deprived of nitrogen and carbon (Scott et al., 1996; Tsukada and Ohsumi, 1993). Nitrogen-starved *Arabadopsis thaliana* autophagy mutants exhibit increased rates of leaf senescence and chlorosis (Doelling et al., 2002). In placental mammals,

Contact information: Jennifer Lippincott-Schwartz, Ph.D, Cell Biology and Metabolism Program, NICHD, NIH, Building 18T, Room 101, 18 Library Drive, Bethesda, MD 20892-5034, Phone: 301 402 1010, Fax: 301 402 0078.
Dale W. Hailey is currently at the University of Washington, Seattle, WA, Peter Kim is at The Hospital for Sick Children, Toronto, Ontario, and Rachid Sougrat is at the King Faisel University, Dammam, Saudi Arabia. All other authors are at the National Institutes of Health, National Institutes of Child Health and Human Development, Cell Biology and Metabolism Program.

autophagy is activated after birth following the switch from placental nourishment to suckling; mice lacking functional autophagy die shortly after birth (Kuma et al., 2004).

An important unanswered question regarding starvation-induced autophagosomes is how these unconventional organelles form. The specific membrane origin of all autophagosomes remains unclear (Juhasz and Neufeld, 2006). Nearly all of the proteins involved in the inception and maturation of autophagosomes are cytosolic proteins that are recruited to membranes (Xie and Klionsky, 2007). Proteomic studies of isolated autophagosomal membranes have identified peripheral proteins but revealed no clear signature of membrane origin (Overbye et al., 2007). Other studies of autophagosome biogenesis have implicated membrane contribution from a number of sources including the ER, TGN, and mitochondria (Axe et al., 2008; Reggiori et al., 2005; Young et al., 2006), raising the possibility that the membrane origin of autophagosomes may be variable. Here, we investigate formation of starvation-induced autophagosomes in a mammalian tissue culture cell model, and uncover a mechanism involving membrane outgrowth from mitochondria outer membranes that is dependent on MFN2 and restricts transfer of most proteins from mitochondria to autophagosomes.

RESULTS

Characteristics of starvation-induced autophagosomes

Starvation-induced autophagosomes were studied in a clonal NRK (Normal Rat Kidney) cell line stably expressing cyan fluorescent protein (CFP) fused to LC3 (line NRK58B). LC3 (formerly MAP1LC3, the rat homolog of *S. cerevisiae Atg8p*) is a canonical marker for autophagosomes. It is covalently attached to phosphatidylethanolamine (PE), which tethers LC3 to autophagic membranes (Kabeya et al., 2000; Mizushima et al., 2004). Under replete growth conditions, CFP-LC3 in line NRK58B was distributed between cytosolic and nuclear pools, with very little CFP-LC3 observed on autophagic membranes (<10 autophagosomes per cell) (Fig. 1A, B, see 0 time point). Replacement of growth media with DPBS (PBS supplemented with glucose, sodium pyruvate, calcium and magnesium), HBSS or serum-free media induced a starvation response; CFP-LC3 was now robustly recruited from the cytosol onto autophagosomal membranes (Fig. 1A). NRK58B cells exhibited very reproducible induction kinetics when maintained at <90% confluence, accumulating on average about 50 CFP-LC3-labeled autophagic structures following a two-hour starvation with DPBS (Fig. 1B).

The starvation-induced, CFP-LC3-labeled structures in NRK58B cells required Vps34/Beclin Class III PI3 kinase activity, one of the most upstream events in autophagosome formation (Furuya et al., 2005). This was demonstrated using 3-methyladenine (3-MA), a potent inhibitor of this kinase complex (Petiot et al., 2000). NRK58B cells starved with DPBS in the presence of 10mM 3-MA failed to recruit CFP-LC3 onto punctae; CFP-LC3 was now distributed predominately in the cytoplasm or nucleus (Fig. 1C middle right, D). Subsequent washout of 3-MA restored the ability of these cells to induce autophagy in response to starvation (Fig. 1C far right, D).

Formation of starvation-induced autophagosomes also exhibited sequential recruitment of mApg5 and LC3. mApg5 is a marker for initial autophagosome formation and is required for subsequent recruitment of LC3 (Mizushima et al., 2001). Using live cell imaging, we observed a rapid accumulation of YFP-mApg5 fluorescent signal, followed by abrupt signal loss at punctae (Fig. 1E, see Supplemental Movie 1). This YFP-mApg5 signal persisted for ~3 minutes, and its release always occurred concurrently with accumulation of CFP-LC3 (Fig. 1E, F). Because of the transient nature of the YFP-mApg5 spots and their appearance at early stages in autophagosome assembly, we used the intracellular locations of these spots

to map sites of autophagosome assembly. Mapping the sites of YFP-mApg5 punctae indicated that autophagosome assembly occurs at sites dispersed throughout the cell rather than at a tightly localized site of assembly (Fig. 1G).

The autophagosomes generated by starvation in the NRK58B cell culture system captured diffuse cytosolic components. This was demonstrated for glyceraldehyde 3-phosphate dehydrogenase (GAPDH), a long-lived cytosolic protein previously reported to be an autophagy substrate (Hoyvik et al., 1991; Sneve et al., 2005). Exogenously expressed GAPDH-YFP (Fig. 1H, PreFLIP) was visualized in nutrient-deprived NRK58B cells. Fluorescent signal from freely diffusing, cytosolic GAPDH-YFP molecules was depleted by repetitive photobleaching targeted to a small region of cytosol. This revealed non-diffusing subpopulations of GAPDH in punctae that co-localized with either lysosomal markers (not shown) or CFP-LC3 (Fig. 1H, PostFLIP), indicating they were autophagosomes with trapped GAPDH-YFP substrate.

To visualize fusion of autophagosomes with lysosomes, autophagosomes and lysosomes were simultaneously imaged. Starved NRK58B were labeled with the lysosomal marker, LysoTracker Red DND-99. Live-cell imaging revealed fusion events between CFP-LC3-labeled autophagosomes and LysoTracker-labeled lysosomes (See Supplemental Movie 2, frames shown in Fig. 2A). Upon fusion, LysoTracker signal accumulated in CFP-LC3-labeled autophagosomes. Soon thereafter, CFP-LC3 signal from these structures was lost (Fig. 2A, see yellow arrow at 3 min). Due to this loss, starved cells showed little overall overlap of CFP-LC3 with LysoTracker (Fig. 2A) or other lysosomal markers, including YFP-Lgp120 (yellow fluorescent protein fused to the LAMP1 rat homolog) (not shown).

The lifetime of the starvation-induced autophagosomes was examined using a pulse-labeling approach using photoactivatable GFP (PA-GFP) (Patterson and Lippincott-Schwartz, 2002). When PA-GFP is exposed to ~400-nm light, its excitation spectra is irreversibly altered to a state where it can be excited by 488-nm light. Non-activated PA-GFP, by contrast, remains dark when imaged with 488-nm light. NRK cells stably expressing PAGFP-LC3 were starved by DPBS treatment, photoactivated, and then tracked by live cell imaging. Starvation-induced autophagosomes exhibited near complete turnover within 40 minutes (Fig. 2B upper panels, C; See Supplemental Movie 3). Loss of PAGFP-LC3 signal was not due to photobleaching or release of PAGFP-LC3 from autophagosomes prior to lysosomal fusion, since the observed loss in signal was blocked by treatment with chloroquine (Fig. 2B lower panels, C), an aminoquinoline that increases intralysosomal pH, inactivates pH-dependent lysosomal proteases, and blocks lysosomal fusion with autophagosomes (Bjorkoy et al., 2005; Tasdemir et al., 2008).

Altogether, these data indicate that starvation-induced autophagosomes in the NRK58B line display classic characteristics of autophagosomes: they require Class III PI3Kinase activity and exhibit subsequent mApg5 and LC3 recruitment. Furthermore, the starvation-induced autophagosomes assemble at sites scattered throughout the cell, capture cytosolic cellular components; and degrade in a lysosomal dependent fashion over a short period of time.

Identifying the membrane source of starvation-induced autophagosomes

To identify the membrane origin of starvation-induced autophagosomes, a battery of YFP-fusion proteins, targeted to different intracellular organelles, were transiently expressed in NRK58B cells. We reasoned that if a particular type of organelle was utilized in the formation of autophagosomes, then chimeric markers targeted to this organelle might be transferred to induced autophagosomes. The markers tested included those for the Golgi apparatus (GalT-YFP), trans Golgi network (TGN38-YFP), early endosomal system (EEA1-YFP), plasma membrane (YFP-GPI), and two related markers targeted to the ER and

mitochondria. One of these consists of YFP fused to the targeting sequence of endoplasmic reticulum cytochrome b5, herein referred to as YFP-ER^{cb5}TM. The other consists of YFP fused to the targeting sequence of a mitochondrial cytochrome b5 isoform, herein referred to as YFP-Mito^{cb5}TM. The mitochondrial cytochrome b5 isoform (expressed throughout the eukaryotic kingdom) differs from the ER isoform in that it has a shorter transmembrane region and positively charged residues at its distal C-terminus. These differences are sufficient and necessary to target this isoform specifically to the mitochondria (Borgese et al., 2001; D'Arrigo et al., 1993; Lederer et al., 1983). We observed that YFP fusions to ER^{cb5}TM and Mito^{cb5}TM expressed in NRK cells co-localized uniquely with ER and mitochondrial markers, respectively. Significantly, there was no YFP-ER^{cb5}TM signal in mitochondrial membranes, and no YFP-Mito^{cb5}TM signal in ER membranes of transfected NRK58B cells, regardless of expression levels (see Supplemental Fig. 1s).

For most of the surveyed organelles (e.g., early endosomes, Golgi, ER and TGN), high-resolution images clearly revealed little or no overlap with CFP-LC3-positive autophagosomes (Fig. 3A--see insets, B). This included the ER marker, YFP-ER^{cb5}TM, where regions of low ER density showed no overlap with CFP-LC3 (Fig. 3A, insets). This same lack of overlap was seen for another ER marker, CD3δ-YFP. Because the ER is continuous, we also used repetitive photobleaching of a small region to deplete signal from the entire ER network. Following bleaching, ER markers were not detected in starvation-induced autophagosomes, suggesting no transfer of ER markers to autophagosomes had taken place. (Supplemental Fig. 2s).

Surprisingly, the only marker to show significant overlap with autophagosomes was the YFP-Mito^{cb5}TM mitochondrial outer membrane marker. YFP-Mito^{cb5}TM was present on nearly 80% of CFP-LC3 positive autophagosomes formed after 2 h of DPBS treatment (Fig. 3A, far right, C). Other markers exhibited much less overlap with autophagosomes (<20% for all other YFP fusions). The associated pool of YFP-Mito^{cb5}TM on autophagic membranes was stably associated with those membranes. This was demonstrated by photobleaching YFP-Mito^{cb5}TM signal within individual cells to deplete all signal except that present on isolated autophagic vesicles. YFP-Mito^{cb5}TM under these conditions showed persistent signal on isolated structures for >3 minutes (Fig. 3C).

Hence, the only organelle marker that autophagosomes co-localized with extensively was the marker for the mitochondrial outer membrane (MOM). Notably, this behavior was specific to starvation. When we applied the same methodology to study overlap of YFP-Mito^{cb5}TM and CFP-LC3 in thapsigargin-treated NRK58B cells, overlap of the MOM marker with autophagosomes was not observed (overlap <10%) (Supplemental Fig 3s).

Autophagosome/mitochondria overlap during starvation is not due to mitophagy

We next asked whether overlap of the YFP-Mito^{cb5}TM mitochondrial outer membrane marker with the autophagic marker was due to induction of mitophagy, a process wherein mitochondria are captured and degraded (Mijaljica et al., 2007). Mitophagy predicts equal or more overlap of matrix and inner membrane mitochondrial markers with CFP-LC3-positive structures compared to an outer membrane marker. Hence, we tested co-localization of other mitochondrial components (i.e., mitochondrial matrix and inner membrane) with CFP-LC3 after autophagic induction. We starved the cells and subsequently quantifying overlap of matrix targeted Mito-YFP (yellow fluorescent protein fused to the targeting sequence of cytochrome c oxidase subunit VIII) and the inner membrane marker 10N-nonyl acridine orange (a cell permeant dye that labels cardiolipin in the inner mitochondrial membrane (Petit et al., 1992) with induced autophagosomes (Fig 4A). Neither of these markers showed a comparable degree of overlap with the autophagasomal marker (9%, 16% respectively compared to 78% for YFP-Mito^{cb5}TM (Fig 4B). Similarly, the inner membrane marker

Prohibitin-YFP also showed dramatically less autophagosome-associated signal (Fig. 4B). Contrary to what mitophagy predicts, therefore, matrix and inner mitochondrial markers did not overlap with CFP-LC3-positive structures induced by starvation.

Mitophagy also predicts that mitochondrial components associated with autophagosomes should be captured inside autophagosomes. To test this, we examined CFP-LC3-labeled autophagosomes in starved NRK58B cells transiently expressing YFP-Mito^{cb5}TM and GAPDH-RFP. High-resolution imaging resolved isolation membranes of autophagosomes around sequestered GAPDH-RFP signal (Fig. 4C). Line profiles of GAPDH-RFP within autophagosomes exhibited single bell-shaped intensity profiles, consistent with soluble protein trapped in the lumen of the autophagosomes. By contrast, YFP-Mito^{cb5}TM showed two well-delineated intensity peaks at the limiting membranes of many autophagic vesicles, as seen for CFP-LC3 (Fig. 4D). This indicated that YFP-Mito^{cb5}TM in autophagosomes was present on the membranes of these organelles, not captured within their lumen.

Finally, when we compared DPBS incubation with conditions reported to induce large-scale mitophagy in our system, we found there were significant differences. Mitophagy can be induced by drug treatments that inhibit pan-caspase activity and simultaneously damage mitochondria (e.g., Z-VAD-FMK/Staurosporine treatment) (Colell et al., 2007). In these conditions, flow cytometry revealed loss of mitochondrial mass in a significant fraction of the population of treated cells. Additionally, in these conditions, we observed autophagosomes in treated NRK58B cells that contained both mitochondrial matrix and inner membrane (see Supplemental Fig. 4s). However, incubation in DPBS produced neither appreciable loss of mitochondrial mass nor apparent capture of entire mitochondria (see Fig. 4 & Supplemental Fig 4s). In our system therefore, we concluded that mitophagy is not the principle event underlying the presence of YFP-Mito^{cb5}TM in autophagosomal membranes during DPBS incubation.

Starvation-induced autophagosomes emerge from sites on mitochondria

We next considered other scenarios that could result in overlap of the mitochondrial outer membrane marker YFP-Mito^{cb5}TM with the autophagy marker. One possibility is that mitochondrial outer membrane is used in autophagosome biogenesis. To test this we performed high-speed, live-cell imaging of NRK cells expressing GFP-LC3 and Mito-RFP in cells that were starved for 1 h. We aimed to visualize any possible outgrowth of autophagosomes from mitochondrial outer membrane.

Strikingly, GFP-LC3 punctae first appeared in association with mitochondria (Fig. 5A, yellow arrows; See Supplemental Movie 4). These punctae retained association with mitochondria over short time periods despite highly dynamic mitochondrial movements. Like GFP-LC3 punctae, signal from another tagged marker (GFP-mApg5) also associated with mitochondrial sites. mApg5 is present in an oligomeric complex (mApg5/Apg12/Apg16); membrane association of this complex is a prerequisite for recruitment of LC3 to membranes(Mizushima et al., 2001). In starved NRK cells transiently expressing GFP-mApg5, highly dynamic GFP-mApg5 punctae appeared along mitochondrial elements (Supplemental Fig. 5s, yellow arrows, Supplemental Movie 5), and persisted along these elements through their lifetime.

Transmission electron microscopy (EM) results further supported mitochondrial membrane involvement in autophagosome formation. EM of DPBS-induced NRK58B and wild type NRK cells revealed the presence of multilamellar, autophagosomal structures that were never observed in unstarved cells. While most of these structures appeared as isolated organelles, some were closely apposed to or continuous with mitochondrial elements (Fig. 5B). The mitochondrial-associated structures excluded mitochondria inner membrane and

matrix and showed a luminal electron density like that of the cytoplasm—suggesting engulfment of cytosol. The dimensions of these structures correlated well with the dimensions of CFP-LC3 positive structures observed by confocal microscopy. To address whether these structures were LC3-positive, starved NRK58B cells were fixed, permeabilized and labeled with gold conjugated antibodies to CFP (Fig. 5C). Clusters of gold label were observed in structures adjacent to mitochondria with the same dimensions as the multilamellar, autophagosomal-looking structures seen by EM alone.

Membrane continuity between outer mitochondrial membrane and newly formed autophagosomes

The above results suggested starvation-induced autophagosomes emerge from mitochondrial outer membranes. If so, then mitochondria and autophagosomes should share membranes at some point during the formation of autophagosomes. We frequently observed CFP-LC3/YFP-Mito^{cb5}TM positive structures present along a YFP-Mito^{cb5}TM-labeled tubular mitochondrion. Because of the limits of optical resolution, high-resolution images alone could not reveal whether YFP-Mito^{cb5}TM positive autophagic vesicles were in close proximity or whether the structures actually shared membrane with associated mitochondria. We used high-speed, high-resolution imaging coupled with targeted laser bleaching to discriminate between these two possibilities. Mitochondrial elements with associated autophagic vesicles were identified. Small regions at the distal ends of associated mitochondrial elements were simultaneously photobleached with 405-nm and 490-nm laser lines. If continuity was present, we predicted YFP signal from both the mitochondria and associated autophagosomes would be depleted; without continuity, only the mitochondrial YFP signal would be depleted (See schematic--Fig. 5D).

Upon repetitive bleaching of a mitochondrial element, YFP-Mito^{cb5}TM signal along the entire length of the targeted mitochondrial element was depleted due to rapid diffusion of the protein in and out of the targeted photobleached region (Fig. 5E,F). Strikingly, in some instances, this photobleaching also depleted YFP-Mito^{cb5}TM from regions of CFP-LC3 overlap outside the photobleached region (Fig. 5E, see arrows, middle panel). Post-translational insertion of YFP-Mito^{cb5}TM directly into the membranes of autophagosomes and close spatial proximity to mitochondrial elements cannot account for these results. The lateral exchange of YFP-Mito^{cb5}TM between mitochondrial elements and regions of CFP-LC3 overlap instead indicates that membrane continuity must exist between the maturing autophagosomal structures and associated mitochondrial elements. This continuity permits rapid diffusion of YFP-Mito^{cb5}TM between associated structures. The majority of autophagosomes did not exhibit this behavior, and it was not observed with large (>800nm) CFP-LC3/YFP-Mito^{cb5}TM positive structures. There, no loss of YFP-Mitocb5TM signal within autophagosomes occurred upon repeated bleaching of a closely associated mitochondrion (Fig 5F). These findings thus suggested that continuity of autophagosome and mitochondria membranes is transient, likely representing an early event in the formation and maturation of starvation-induced autophagosomes.

Lipid delivery from mitochondria to newly forming autophagosomes

If mitochondrial outer membranes serve as a membrane source for autophagosome formation, then lipid components of mitochondrial outer membranes should be found in autophagosomal membranes. There are no known lipid markers that uniquely label the outer mitochondrial membrane. However, we took advantage of the now well-established transfer of lipids from the ER to the mitochondria. Phosphotidylserine (PS), in particular, is readily transferred from the ER to mitochondria where it is converted to phosphotidylethanolamine (PE) by activity of the mitochondrial enzyme, phosphotidylserine decarboxylase (Vance and Vance, 2004). To see if lipid is transferred between mitochondrial and autophagosomal

membranes, we loaded cells with 18:1-06:0 NBD phosphotidylserine (NBD-PS)--a fluorescent analog of phosphotidylserine that previously has been shown to label mitochondria after transfer from the ER (Kobayashi T and Arakawa Y, 1991). We observed fluorescent signal from NBD-PS first in ER membranes and later in mitochondrial membranes (Fig. 6A, B). When cells exhibiting mitochondrial labeling were starved, NBD fluorescence subsequently appeared in starvation-induced autophagosomes (Fig 6C). Furthermore, NBD fluorescence in autophagosomes was increased by treatment with drugs that disrupt fusion of autophagosomes with lysosomes (data not shown). This data suggested the NBD probe was transferred from mitochondria to autophagosomes. As this is consistent with the behavior of the protein marker YFP-Mito^{cb5}TM, the results further supported a role for mitochondrial membranes in the formation of autophagosomes.

Cells lacking mitofusin 2 do not form autophagosomes in response to starvation

As further evidence for mitochondrial membrane involvement in autophagy, we followed up on the above observation that mitochondrial lipid (which had originated in the ER) is transferred to autophagosomes in starved cells. We reasoned that if this is crucial for making autophagosomes in starved cells, then blocking contact of mitochondria with ER to impede lipid transfer might inhibit starvation-induced autophagy. To test this possibility, we used a cell line lacking mitofusin 2 (Mfn2), a mitochondrial fusion factor recently shown to help tether mitochondria to ER (de Brito and Scorrano, 2008). YFP-LC3 was transiently transfected into the MFN2−/− cells and control cells. The cells were then starved for 2h and examined by confocal microscopy. Whereas robust autophagic induction occurred in control cells, no induction occurred in cells lacking Mfn2 (Fig. 6D,E). These results indicate that Mfn2 tethering activity is necessary for starvation-induced autophagosomes to form, and support the idea that membrane lipids of autophagosomes (which are PE enriched) derive from mitochondria in starved cells.

Mitochondrial proteins are largely excluded from autophagosomes

Close contacts of mitochondria with ER could serve to re-supply lipid to mitochondria to compensate for lipid transfer into autophagosomes during starvation. But what prevents protein components from being depleted from mitochondria during starvation? To address this, we examined whether transfer of proteins from outer mitochondrial membrane to autophagosomes was selective. We found this to be the case. Unlike Mito^{cb5}TM, outer mitochondrial membrane proteins with transmembrane anchors that span the outer membrane bilayer (e.g., Tom20, Mfn2, and Fis1), showed no transfer into autophagosomes induced by starvation (Fig. 7A). Thus, key mitochondrial outer membrane proteins (in addition to mitochondrial matrix and inner membrane proteins (see Fig. 4B)) are excluded from autophagosomes formed in starved cells.

How might some outer mitochondrial membrane proteins (e.g., Fis1 and Tom20) but not others (Mito^{cb5}TM) be excluded from autophagosomes? Sharp curvature is known to lead to selectivity in protein transfer due to steric and topological constraints in the region of high curvature (Schmidt and Nichols, 2004). We considered the possibility, therefore, that a selective barrier at the site of autophagosomal membrane budding might explain why many mitochondrial proteins are excluded from entering autophagosomes (see Fig. 7B for schematic of highly curved membranes). Previous studies of the ER isoform of cb5 identified a proline in the transmembrane domain that allows for formation of a kinked helix. Based on crosslinking and photochemistry studies, this kinked helix form can intercalate into only the outer leaflet of the targeted bilayer (Takagaki et al., 1983; Vergeres and Waskell, 1995) (see Fig. 7C). We speculated that this single leaflet interaction might explain the ability of the YFP-Mito^{cb5}TM marker to diffuse into forming autophagosomes.

To test this idea, we altered the transmembrane domain of the YFP-Mito^{cb5}TM. Conversion of a specific proline to alanine in the cb5 transmembrane domain was previously shown to force the domain into a linear helical coil that spans both leaflets of the target membrane (Vergeres and Waskell, 1995). Given this precedent, we constructed an alanine mutant of YFP-Mito^{cb5}TM(P115A) and tested this marker to see if it was distributed on autophagosomes as well as mitochondria in starved cells. When expressed in NRK58B cells, the alanine mutant YFP-Mito^{cb5}TM(P115A) was efficiently targeted to the mitochondria. However, in DPBS-treated cells it was not observed on induced autophagosomes (Fig. 7D,E). The degree of co-localization with autophagosomes was strikingly different than wild-type YFP-Mito^{cb5}TM, and equivalent to the degree of overlap observed for the matrix marker (see Fig 4C) and for another transmembrane marker associated with the outer membrane (YFP-Mito^{Fis1}TM) (see Fig. 7A).

Exclusion of the YFP-Mito^{cb5}TM(P115A) mutant from autophagosome membranes supports the mechanism proposed here for how most mitochondrial proteins could be excluded from autophagosomal membranes. In this mechanism, only proteins associating with the outer leaflet of the outer mitochondrial membrane, like YFP-Mito^{cb5}TM, can traverse the point of sharp curvature imposed by autophagosome biogenesis. This could underlie the paucity of integral membrane proteins observed in autophagosomal membranes (Fengsrud et al., 2000). Additionally, the closely apposed membranes of autophagic vesicles could exclude proteins present in the inner-membrane space.

DISCUSSION

A number of reports suggest that there is a connection between mitochondria and autophagosome formation. Several autophagy proteins (e.g., Beclin-1, the yeast protein Atg9p, a proteolytic fragment of Atg5, and Bif-1) have been previously localized to mitochondria (Reggiori et al., 2005; Takahashi et al., 2007b; Yousefi et al., 2006). Additionally, several mitochondrial-localized proteins (e.g., smARF, Bif-1/EndophillinB) positively regulate autophagy (Lee et al., 2008; Reef et al., 2006; Takahashi et al., 2007a). Knockdown of Bif-1 (a Bax-binding protein that also binds the Class III PI3Kinase complex) suppresses induction of autophagy during starvation, as does knockdown of Sirt1, a deacetylase that regulates mitochondrial biogenesis by deacetylating PGC1α. While reports of interplay between autophagy and mitochondria are often ascribed to mitophagy, our data suggest an alternative—that mitochondria participate in the formation of autophagosomes. Here, we show that autophagosome inception occurs along mitochondria. The early autophagosomal marker mApg5 transiently localizes to punctae on the mitochondria. LC3 subsequently replaces mApg5 at these sites where LC3-positive autophagosomes transiently associate with mitochondria. We show that a tail-anchored outer mitochondrial membrane protein labels the membranes of autophagosomes, and that its delivery to autophagosomal membranes is via the mitochondria membrane. We demonstrate this marker can be depleted from autophagosomes by photobleaching associated mitochondrial elements; therefore the membranes of these organelles are transiently shared. We further show that a mitochondrial lipid probe is conveyed from mitochondria to autophagosomes. Tomography and immuno EM further reveal autophagic structures associated with mitochondria that exclude mitochondrial matrix and inner membrane. Finally, we show that no autophagosome induction during starvation occurs in cells lacking MFN2, a mitochondrial protein involved in tethering of mitochondria to ER.

Formation of autophagosomes from the outer mitochondrial membrane requires delivery of the most upstream autophagic factors to the mitochondrial membrane. Consistent with this, Beclin-1 (a component of the Vps34/Beclin Class III PI3Kinase complex) has been reported on mitochondria. One plausible scenario by which multilamellar structures could derive

from the outer membrane involves recruiting autophagy machinery to the mitochondria in order to impose membrane curvature on the outer mitochondrial membrane (see schematic, Fig. 7F). The Vps34/Beclin complex may mark an initiation site. Phosphorylation of the target phosphoinositide and Bif-1 BAR domain interactions with membrane could create and stabilize a microdomain that subsequently recruits the mApg5/Atg12/Atg16 complex. Oligomerization of this complex (reported in (Kuma et al., 2002;Mizushima et al., 2003) could then form a transient coat and expand the initiation site. LC3 conjugation to phosphotidylethanolamine (PE) at the site could stabilize local high concentrations of PE in the outer leaflet of the mitochondria outer membrane and support continued outgrowth of a structure. Notably, PE is one of a small set of lipids that imposes a negative radius of curvature, favoring formation of a cup-like structure that could capture cytosol within its volume (Thomas and Poznansky, 1989;van Meer et al., 2008). A multi-lamellar structure could then form if the distal edges fused. LC3 has been shown to catalyze fusion of homotypic membranes in an *in vitro* system (Nakatogawa et al., 2007). Such a scenario is consistent with the known activities of core autophagy machinery, and would allow for the establishment of asymmetric lipid composition from an existing membrane source to promote membrane curvature.

Given the ability of autophagy machinery to target a membrane, establish a stable microdomain, and promote membrane curvature, autophagosomes could potentially form from a variety of sources. Core autophagy machinery, which is almost entirely cytosolic, has been reported to target membranes of different origins. While ER stress-induced autophagosomes appear to utilize ER membrane (Bernales et al., 2006), other reports have recently demonstrated that the autophagy protein LC3 can also be recruited to membranes derived from the plasma membrane (Sanjuan et al., 2007). We therefore postulated that inducing autophagy in our line by another stress might produce autophagosomes with characteristics that are distinct from autophagosomes induced by starvation. A number of conditions have been reported to induce autophagy, including ER stress. When we treated NRK58B cells with the ER calcium pump inhibitor thapsigargin to perturb the ER folding environment (Brostrom and Brostrom, 2003, Tadini-Buoninsegni et al., 2008), CFP-LC3 positive structures were robustly generated, consistent with other reports or ER stress-induced autophagy (Ogata et al., 2006; Sakaki et al., 2008). Notably, thapsigargin induced structures were sensitive to 3-MA. However, they did not label with YFP-Mito^{cb5}TM (see Supplemental Fig. 3s). Utilization of different membranes in autophagosome biogenesis thus may produce different classes of autophagosomes, resulting in autophagic structures with behaviors specific to their induction conditions (see Supplemental Fig 6s). We favor the idea that the question of what membrane is utilized collapses to a question of how autophagosome assembly is initiated at diverse sites.

Why might starvation specifically utilize mitochondrial membrane? A little-explored aspect of autophagy is its potential role in fluxing lipids through otherwise disconnected cellular compartments. Our photochase data employing LC3 tagged with photoactivatable GFP indicates that a significant amount of membrane is moving from the autophagosomal origin to autolysosomes/lysosomes via fusion of outer autophagosomal membranes with lysosomal membranes. The lipid target of LC3—phosphotidylethanolamine—is an abundant cellular lipid that is transferred by autophagosomes. PE is synthesized principally at two sites—in the ER via the CDP-ethanolamine pathway and in the mitochondria via decarboxylation of phosphotidylserine (Vance, 2008). ER synthesis of PE utilizes DAG and exogenous ethanolamine. By contrast, synthesis in the mitochondria utilizes phosphotidylserine transferred from the ER. Under starvation conditions the sources for exogenous ethanolamine and DAG (produced following growth factor engagement) are restricted. These substrates are required for PE synthesis in the ER. Autophagy may counter this by routing mitochondrial-derived PE to lysosomes, and subsequently via retrograde transport,

back through the secretory pathway. Mitochondria contribution to autophagosomal membranes under starvation conditions may therefore contribute to lipid homeostasis in addition to established roles in nutrient recycling.

Given a significant flux of lipid, one prediction of utilizing mitochondrial lipids is a depletion of mitochondria. However, starvation-induced autophagy does not result in net loss of mitochondrial mass in our system. In fact, mitochondrial mass increases slightly with increased incubation time in DPBS. Other conditions reported to induce autophagy (i.e., Sirt1 overexpression) similarly show concurrent autophagosome proliferation and increased mitochondrial mass (Lee et al., 2008). How might mitochondrial mass be maintained? Notably, a major source for mitochondrial phospholipids is the ER. Mitochondrial-associated membranes (MAM's) act as bridges between the mitochondria and ER in both yeast and mammals, where phosphotidylserine and other phospholipids are transferred to mitochondria (Achleitner et al., 1999; Bozidis et al., 2008). An unexplored question is whether autophagy promotes transfer of lipid from the ER to mitochondria. We have evaluated whether ER/mitochondrial connections are important for autophagic induction. de Brito and Scorrano recently reported that loss of mitofusin2 disrupts connections between the ER network and mitochondria. We found that mitofusin2 knockout cells fail to produce autophagosomes when starved. Therefore, there appears to be a requirement for lipid contribution from the ER to mitochondria in order for starvation-induced autophagy to proceed.

Work by Axe et al reported that DFCP1, a unique PI3(P) binding protein in the ER, translocates to punctae under starvation that label sites where autophagosome formation occurs (Axe et al., 2008). The authors observe mApg5 and LC3 autophagosomal markers surrounded by DFCP1, and present a model suggesting autophagosomes form from ER membrane at these sites. Our data suggest another possibility—that DFCP1 sites may be sites of connection between the ER and mitochondria that respond to starvation conditions. Conditions that induce the very rapid formation of autophagosomes may drive transfer of lipid from the ER to the mitochondria where these lipids are subsequently modified and utilized in autophagosome biogenesis without affecting mitochondrial mass.

Whether autophagosomes form *de novo* or from pre-existing cytomembranes is a long-standing debate, and investigating how autophagosome assembly is initiated and proceeds remains difficult (Juhasz and Neufeld, 2006). The findings presented here indicate that mitochondria participate directly in the formation of autophagosomes while retaining mitochondrial proteins by diffusion barriers. This utilization of the outer membrane of the mitochondria defines a new intracellular pathway from mitochondria to the autophagosomal/lysosomal system. Budding of vesicles from mitochondria that transit to peroxisomes has been reported (Neuspiel et al., 2008). Such events, together with the mitochondrial pathway to autophagosomes reported here, may underlie the constitutive movement of mitochondrial-derived factors (e.g., heme (Rajagopal et al., 2008)) to different cellular locations, and implicate mitochondrial involvement in as yet unappreciated aspects of cell biology.

EXPERIMENTAL PROCEDURES

Plasmid Constructs

Plasmid information and constructions are outlined in Supplemental Data.

Cell Culture

For maintenance, cells were grown in DMEM/10% FBS/Penn/Strep. Clonal cell lines were selected with 800ug/mL G418. For live cell imaging, cells were grown in LabTek chambers with #1 borosillicate cover glass (Nalge Nunc International, Naperville, IL) 16 hours prior to

imaging and maintained in CO2 independent media (Invitrogen, Carlsbad, CA) or appropriate media formulations at the scope. Transfections were done with Fugene 6 reagent (Roche, Indianapolis, IN) 16 hours prior to imaging.

Media treatments

Starvation was induced by incubation in DPBS with D-glucose and sodium pyruvate (Invitrogen SKU# 14287-080), or, where noted, serum-free DMEM or HBSS.

Fluorescence Microscopy

Images were aquired on Zeiss LSM 510 Meta, Zeiss LSM DUO, and Perkin Elmer UltraView ERS 6FO-US systems. (See supplemental data for hardware specifications and further details.) Digital images were analyzed using either LSM (Carl Zeiss MicroImaging, Inc.) or ImageJ (NIH/public domain) software. Images were adjusted for brightness and contrast using Photoshop CS (Adobe). For movies, time-lapse sequences were converted to directories of tif images. Identical adjustments were applied to all frames using the Photoshop batch function; directories were reassembled into movie files using QuickTime Pro.

Live Cell Staining

LysoTracker DND99, and Mitotracker RedCMXRos (Invitrogen Molecule Probes) were added directly to media at 100nM and 150nM respectively, incubated for 10 minutes, and subsequently washed immediately before imaging. For NBD-PS labeling, NBD-PS was reconstituted to a 2.2mM stock in sterile PBS and added to cells at a 0.22mM final concentration for 30 minutes. See supplemental materials for lipid formulation.

Pharmaceutical treatments

3-Methyladenine was purchased from Sigma (Cat M9281-100MG) and used at 10mM. Thapsigargin was purchased from Sigma (Cat T9033) and used at 25nM. Digitonin was purchased from Calbiochem (Cat 300410) and used at 1:1000 of a 6% stock solution. KHM buffer is described in (Lorenz et al., 2006). Chloroquine was purchased from Sigma and used at 1:100 of a 100uM stock solution. Z-VAD-FMK and Staurosporine were purchased from Sigma (Cat# V-116 and S6942 respectively.) See Supplemental data for further details.

Flow Cytometry

Cells plated on tissue culture dishes were stained with Mitotracker green FM (100nM for 30 mins) and subsequently washed three times with pre-equilibrated media. Cells were then trypsinized, centrifuged at 300g, and washed twice in medium. Stained cells were diluted in medium and loaded into a BD FACSCalibur FACS flow system (BD Biosciences, San Jose, CA). Data were appropriately gated and analyzed by CellQuest Pro software.

Electron Microscopy

Cells were fixed with 2.5 % glutaraldehyde in 0.1 M Cacodylate buffer, and post-fixed in reduced osmium prior to Epon embedding. 70 to 100nm sections were cut and collected on carbon-coated grids and subsequently stained with lead citrate. Grids were imaged with a Tecnai 20 TEM (FEI Company, Netherlands) operating at 120 kV. Images were captured on a 2k × 2k CCD camera (Gatan, Pleasanton, CA, USA). For ImmunoEM, cells were fixed in 4% paraformaldehyde and blocked with 1% bovine serum albumin in PBS. Permeabilized cells (0.05 % saponin in PBS/BSA 1%) were incubated with primary GFP antibody (rabbit anti-GFP; Molecular Probes), washed, and subsequently incubated with nanogold-conjugated secondary antibodies (Nanoprobes). Cells were then fixed with glutaraldehyde, treated with a gold enhancement mixture for 6 min and post-fixed in reduced osmium prior

to embedding in Epon. 70 to100 nm sections were cut and stained with lead citrate prior to imaging.

Supplementary Material

Refer to Web version on PubMed Central for supplementary material.

Acknowledgments

We thank Yoshinori Ohsumi, Noboru Mizushima, Heidi McBride, Richard Youle, Manoj Raje, Holger Lorenz, and Christian Wunder for sharing reagents. We thank David C. Chan for the $Mfn2^{+/+}$ and $Mfn2^{-/-}$ MEF cells. We also thank Heidi McBride and Richard Youle for helpful comments and Timothy Mrozek for assistance with illustrations.

References

Achleitner G, Gaigg B, Krasser A, Kainersdorfer E, Kohlwein SD, Perktold A, Zellnig G, Daum G. Association between the endoplasmic reticulum and mitochondria of yeast facilitates interorganelle transport of phospholipids through membrane contact. Eur J Biochem. 1999; 264:545–53. [PubMed: 10491102]

Axe EL, Walker SA, Manifava M, Chandra P, Roderick HL, Habermann A, Griffiths G, Ktistakis NT. Autophagosome formation from membrane compartments enriched in phosphatidylinositol 3−phosphate and dynamically connected to the endoplasmic reticulum. J Cell Biol. 2008; 182:685–701. [PubMed: 18725538]

Bernales S, McDonald KL, Walter P. Autophagy counterbalances endoplasmic reticulum expansion during the unfolded protein response. PLoS Biol. 2006; 4:e423. [PubMed: 17132049]

Bjorkoy G, Lamark T, Brech A, Outzen H, Perander M, Overvatn A, Stenmark H, Johansen T. p62/SQSTM1 forms protein aggregates degraded by autophagy and has a protective effect on huntingtin −induced cell death. J Cell Biol. 2005; 171:603–14. [PubMed: 16286508]

Borgese N, Gazzoni I, Barberi M, Colombo S, Pedrazzini E. Targeting of a tail−anchored protein to endoplasmic reticulum and mitochondrial outer membrane by independent but competing pathways. Mol Biol Cell. 2001; 12:2482–96. [PubMed: 11514630]

Bozidis P, Williamson CD, Colberg−Poley AM. Mitochondrial and secretory human cytomegalovirus UL37 proteins traffic into mitochondrion−associated membranes of human cells. J Virol. 2008; 82:2715–26. [PubMed: 18199645]

Colell A, Ricci JE, Tait S, Milasta S, Maurer U, Bouchier−Hayes L, Fitzgerald P, Guio−Carrion A, Waterhouse NJ, Li CW, Mari B, Barbry P, Newmeyer DD, Beere HM, Green DR. GAPDH and autophagy preserve survival after apoptotic cytochrome c release in the absence of caspase activation. Cell. 2007; 129:983–97. [PubMed: 17540177]

D'Arrigo A, Manera E, Longhi R, Borgese N. The specific subcellular localization of two isoforms of cytochrome b5 suggests novel targeting pathways. J Biol Chem. 1993; 268:2802–8. [PubMed: 8428954]

Doelling JH, Walker JM, Friedman EM, Thompson AR, Vierstra RD. The APG8/12−activating enzyme APG7 is required for proper nutrient recycling and senescence in Arabidopsis thaliana. J Biol Chem. 2002; 277:33105–14. [PubMed: 12070171]

Fengsrud M, Erichsen ES, Berg TO, Raiborg C, Seglen PO. Ultrastructural characterization of the delimiting membranes of isolated autophagosomes and amphisomes by freeze−fracture electron microscopy. Eur J Cell Biol. 2000; 79:871–82. [PubMed: 11152279]

Furuya N, Yu J, Byfield M, Pattingre S, Levine B. The evolutionarily conserved domain of Beclin 1 is required for Vps34 binding, autophagy and tumor suppressor function. Autophagy. 2005; 1:46–52. [PubMed: 16874027]

Hoyvik H, Gordon PB, Berg TO, Stromhaug PE, Seglen PO. Inhibition of autophagic−lysosomal delivery and autophagic lactolysis by asparagine. J Cell Biol. 1991; 113:1305–12. [PubMed: 1904444]

Juhasz G, Neufeld TP. Autophagy: a forty−year search for a missing membrane source. PLoS Biol. 2006; 4:e36. [PubMed: 16464128]

Kabeya Y, Mizushima N, Ueno T, Yamamoto A, Kirisako T, Noda T, Kominami E, Ohsumi Y, Yoshimori T. LC3, a mammalian homologue of yeast Apg8p, is localized in autophagosome membranes after processing. Embo J. 2000; 19:5720–8. [PubMed: 11060023]

Kuma A, Hatano M, Matsui M, Yamamoto A, Nakaya H, Yoshimori T, Ohsumi Y, Tokuhisa T, Mizushima N. The role of autophagy during the early neonatal starvation period. Nature. 2004; 432:1032–6. [PubMed: 15525940]

Kuma A, Mizushima N, Ishihara N, Ohsumi Y. Formation of the approximately 350−kDa Apg12−Apg5.Apg16 multimeric complex, mediated by Apg16 oligomerization, is essential for autophagy in yeast. J Biol Chem. 2002; 277:18619–25. [PubMed: 11897782]

Lederer F, Ghrir R, Guiard B, Cortial S, Ito A. Two homologous cytochromes b5 in a single cell. Eur J Biochem. 1983; 132:95–102. [PubMed: 6840088]

Lee IH, Cao L, Mostoslavsky R, Lombard DB, Liu J, Bruns NE, Tsokos M, Alt FW, Finkel T. A role for the NAD−dependent deacetylase Sirt1 in the regulation of autophagy. Proc Natl Acad Sci U S A. 2008; 105:3374–9. [PubMed: 18296641]

Lorenz H, Hailey DW, Lippincott−Schwartz J. Fluorescence protease protection of GFP chimeras to reveal protein topology and subcellular localization. Nat Methods. 2006; 3:205–10. [PubMed: 16489338]

Mijaljica D, Prescott M, Devenish RJ. Different fates of mitochondria: alternative ways for degradation? Autophagy. 2007; 3:4–9. [PubMed: 16929167]

Mizushima N, Kuma A, Kobayashi Y, Yamamoto A, Matsubae M, Takao T, Natsume T, Ohsumi Y, Yoshimori T. Mouse Apg16L, a novel WD−repeat protein, targets to the autophagic isolation membrane with the Apg12−Apg5 conjugate. J Cell Sci. 2003; 116:1679–88. [PubMed: 12665549]

Mizushima N, Yamamoto A, Hatano M, Kobayashi Y, Kabeya Y, Suzuki K, Tokuhisa T, Ohsumi Y, Yoshimori T. Dissection of autophagosome formation using Apg5−deficient mouse embryonic stem cells. J Cell Biol. 2001; 152:657–68. [PubMed: 11266458]

Mizushima N, Yamamoto A, Matsui M, Yoshimori T, Ohsumi Y. In vivo analysis of autophagy in response to nutrient starvation using transgenic mice expressing a fluorescent autophagosome marker. Mol Biol Cell. 2004; 15:1101–11. [PubMed: 14699058]

Nakatogawa H, Ichimura Y, Ohsumi Y. Atg8, a ubiquitin−like protein required for autophagosome formation, mediates membrane tethering and hemifusion. Cell. 2007; 130:165–78. [PubMed: 17632063]

Neuspiel M, Schauss AC, Braschi E, Zunino R, Rippstein P, Rachubinski RA, Andrade−Navarro MA, McBride HM. Cargo−selected transport from the mitochondria to peroxisomes is mediated by vesicular carriers. Curr Biol. 2008; 18:102–8. [PubMed: 18207745]

Patterson GH, Lippincott−Schwartz J. A photoactivatable GFP for selective photolabeling of proteins and cells. Science. 2002; 297:1873–7. [PubMed: 12228718]

Petiot A, Ogier−Denis E, Blommaart EF, Meijer AJ, Codogno P. Distinct classes of phosphatidylinositol 3′−kinases are involved in signaling pathways that control macroautophagy in HT−29 cells. J Biol Chem. 2000; 275:992–8. [PubMed: 10625637]

Petit JM, Maftah A, Ratinaud MH, Julien R. 10N−nonyl acridine orange interacts with cardiolipin and allows the quantification of this phospholipid in isolated mitochondria. Eur J Biochem. 1992; 209:267–73. [PubMed: 1396703]

Rajagopal A, Rao AU, Amigo J, Tian M, Upadhyay SK, Hall C, Uhm S, Mathew MK, Fleming MD, Paw BH, Krause M, Hamza I. Haem homeostasis is regulated by the conserved and concerted functions of HRG−1 proteins. Nature. 2008; 453:1127–31. [PubMed: 18418376]

Reef S, Zalckvar E, Shifman O, Bialik S, Sabanay H, Oren M, Kimchi A. A short mitochondrial form of p19ARF induces autophagy and caspase−independent cell death. Mol Cell. 2006; 22:463–75. [PubMed: 16713577]

Reggiori F, Shintani T, Nair U, Klionsky DJ. Atg9 cycles between mitochondria and the pre−autophagosomal structure in yeasts. Autophagy. 2005; 1:101–9. [PubMed: 16874040]

Sanjuan MA, Dillon CP, Tait SW, Moshiach S, Dorsey F, Connell S, Komatsu M, Tanaka K, Cleveland JL, Withoff S, Green DR. Toll−like receptor signalling in macrophages links the autophagy pathway to phagocytosis. Nature. 2007; 450:1253–7. [PubMed: 18097414]

Schmidt K, Nichols BJ. A barrier to lateral diffusion in the cleavage furrow of dividing mammalian cells. Curr Biol. 2004; 14:1002–6. [PubMed: 15182674]

Scott SV, Hefner−Gravink A, Morano KA, Noda T, Ohsumi Y, Klionsky DJ. Cytoplasm−to−vacuole targeting and autophagy employ the same machinery to deliver proteins to the yeast vacuole. Proc Natl Acad Sci U S A. 1996; 93:12304–8. [PubMed: 8901576]

Sneve ML, Overbye A, Fengsrud M, Seglen PO. Comigration of two autophagosome−associated dehydrogenases on two−dimensional polyacrylamide gels. Autophagy. 2005; 1:157–62. [PubMed: 16874067]

Takagaki Y, Radhakrishnan R, Gupta CM, Khorana HG. The membrane−embedded segment of cytochrome b5 as studied by cross−linking with photoactivatable phospholipids. J Biol Chem. 1983; 258:9128–35. [PubMed: 6348039]

Takahashi Y, Coppola D, Matsushita N, Cualing HD, Sun M, Sato Y, Liang C, Jung JU, Cheng JQ, Mul JJ, Pledger WJ, Wang HG. Bif−1 interacts with Beclin 1 through UVRAG and regulates autophagy and tumorigenesis. Nat Cell Biol. 2007a; 9:1142–51. [PubMed: 17891140]

Takahashi Y, Coppola D, Matsushita N, Cualing HD, Sun M, Sato Y, Liang C, Jung JU, Cheng JQ, Mule JJ, Pledger WJ, Wang HG. Bif−1 interacts with Beclin 1 through UVRAG and regulates autophagy and tumorigenesis. Nat Cell Biol. 2007b; 9:1142–51. [PubMed: 17891140]

Tasdemir E, Galluzzi L, Maiuri MC, Criollo A, Vitale I, Hangen E, Modjtahedi N, Kroemer G. Methods for assessing autophagy and autophagic cell death. Methods Mol Biol. 2008; 445:29–76. [PubMed: 18425442]

Thomas PD, Poznansky MJ. Curvature and composition−dependent lipid asymmetry in phosphatidylcholine vesicles containing phosphatidylethanolamine and gangliosides. Biochim Biophys Acta. 1989; 978:85–90. [PubMed: 2914133]

Tsukada M, Ohsumi Y. Isolation and characterization of autophagy−defective mutants of Saccharomyces cerevisiae. FEBS Lett. 1993; 333:169–74. [PubMed: 8224160]

van Meer G, Voelker DR, Feigenson GW. Membrane lipids: where they are and how they behave. Nat Rev Mol Cell Biol. 2008; 9:112–24. [PubMed: 18216768]

Vance JE. Phosphatidylserine and phosphatidylethanolamine in mammalian cells: two metabolically related aminophospholipids. J Lipid Res. 2008; 49:1377–87. [PubMed: 18204094]

Vance JE, Vance DE. Phospholipid biosynthesis in mammalian cells. Biochem Cell Biol. 2004; 82:113–28. [PubMed: 15052332]

Vergeres G, Waskell L. Cytochrome b5, its functions, structure and membrane topology. Biochimie. 1995; 77:604–20. [PubMed: 8589071]

Xie Z, Klionsky DJ. Autophagosome formation: core machinery and adaptations. Nat Cell Biol. 2007; 9:1102–9. [PubMed: 17909521]

Young AR, Chan EY, Hu XW, Kochl R, Crawshaw SG, High S, Hailey DW, Lippincott−Schwartz J, Tooze SA. Starvation and ULK1−dependent cycling of mammalian Atg9 between the TGN and endosomes. J Cell Sci. 2006; 119:3888–900. [PubMed: 16940348]

Yousefi S, Perozzo R, Schmid I, Ziemiecki A, Schaffner T, Scapozza L, Brunner T, Simon HU. Calpain−mediated cleavage of Atg5 switches autophagy to apoptosis. Nat Cell Biol. 2006; 8:1124–32. [PubMed: 16998475]

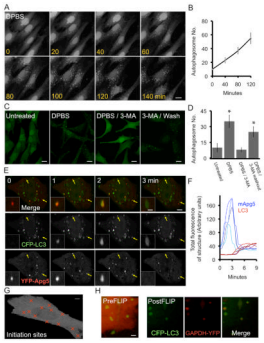

Figure 1. Characterizing the formation of starvation-induced autophagosomes

(A) Time-lapse live-cell imaging of starved NRK58B cells. CFP-LC3 positive structures rapidly proliferated following switch to starvation media. Note concurrent depletion of cytosolic and nuclear pools of CFP-LC3. Growth media (time 0) was replaced with starvation media (subsequent panels). (Scale bar: 20μm) **(B)** Quantification of CFP-LC3 positive structures. Autophagosomes were counted in sequential time-lapse frames and plotted as a function of time in starvation media. Data points show the mean average of 20 cells; error bars show 1 SD **(C)** Treatment with Class III PI(3) kinase inhibitor, 3-methyladenine (3-MA). Robust formation of CFP-LC3 structures required activity of the kinase. Identical wells were untreated, starved, or starved in the presence of the 3-MA for 2 h (three left panels). Subsequently, starved cells treated with 3-MA were washed, incubated in DPBS and imaged 2 h later (right-most panel). 3-MA treatment abolished recruitment of CFP-LC3 to membranes and depletion of cytosolic and nuclear pools (2nd from right). Washout of 3-MA restored ability of cells to induce autophagosome formation during starvation. (Scale bar: 20μm) **(D)** Quantification of 3-MA treatments (mean average of 20 cells +/− 1 SD). Asterisk in bar graphs indicates treatment statistically different from untreated cells by Student t-test: p values < 0.001. **(E)** Time-lapse live-cell imaging of NRK58B cells expressing YFP-mApg5. During starvation, YFP-mApg5 punctae appeared, and subsequently recruited CFP-LC3 and released YFP-mApg5. Arrows indicate two examples. Inset indicates zoom of autophagosome by lower right arrow. See also supplemental Movie 1. (Scale bars: 2μm in inset; 10μm in panel) **(F)** Quantification of YFP-mApg5 and CFP-LC3 signals in time-lapse frames. Dramatic accumulation of YFP-mApg5 always preceded CFP-LC3 recruitment. YFP-mApg5 persisted <4 min and abruptly released. **(G)** Mapping sites of autophagosome formation. The transient appearance of YFP-mApg5 punctae that precedes CFP-LC3 recruitment were scattered throughout the cytosol during starvation. (Scale bar: 5μm) **(H)** Identifying capture of cytosolic proteins in starvation-induced autophagosomes. Freely diffusing signal was depleted by repetitive photobleaching outside the panel region. This depletion revealed a subpopulation of GAPDH-YFP captured within CFP-LC3 labeled structures. (Scale bar: 2μm).

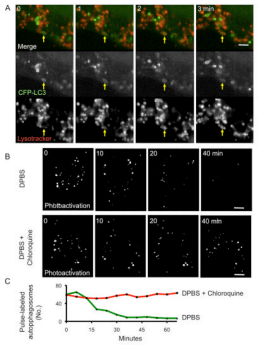

Figure 2. Characterizing the fate of starvation induced autophagosomes

(A) Visualizing fusion of autophagosomes with lysosomes. NRK58B cells were starved and subsequently labeled with a cell permeant vital lysosomal marker. Live-cell imaging revealed fusion events between autophagosomes and lysosomes that caused accumulation of lysosomal marker and coincident loss of CFP-LC3 signal from the autolysosome (arrow). See also supplemental Movie 2. **(B)** Visualizing turnover of autophagosomes by photo pulse-labeling and live cell imaging. Following a 2 h starvation, PAGFP-LC3 cells were photoactivated and depleted of cytosolic activated signal to pulse-label an existing population of autophagosomes (Top left panel). Live cell imaging revealed time dependent disappearance of the pulse-labeled population (top panels; see also supplemental Movie 3), which was blocked by addition of chloroquine. **(C)** Quantification of the lifetime of the structures. Note the turnover of starvation-induced autophagosomes was surprisingly efficient: $t_{1/2}$ of ~25 minutes.

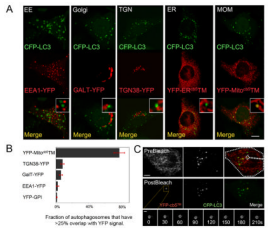

Figure 3. Evaluating exogenous membrane-targeted markers for transfer to autophagosomes

(A) Expression of chimeric-YFP membrane markers in starvation induced NRK58B cells. Chimeric YFP markers targeting intracellular membrane systems were expressed in NRK58B cells (shown left to right: early endosomal system, Golgi, trans Golgi network, ER, and mitochondrial outer membrane). The mitochondrial outer membrane marker, YFP-Mito^{cb5}TM, uniquely co-localized with induced autophagosomes. (Scale bar: 15μm) **(B)** Quantification of overlap of CFP-LC3 signal with membrane marker signal. For each marker, autophagosomes with greater than 25% CFP signal overlap with YFP signal were counted; this number was divided by the total number of autophagosomes to determine percent of total autophagosomes that overlapped with marker. The mean average of twenty cells is shown +/− 1 SD. **(C)** Assessment of the stability of YFP-Mito^{cb5}TM on autophagosomal membranes. YFP-Mito^{cb5}TM-positive autophagosomes were identified. YFP-Mito^{cb5}TM was subsequently bleached in the remainder of the cell (photobleached region indicated by hashed line, top right panel). Unbleached YFP-Mito^{cb5}TM signal persisted on autophagosomes (time series in seconds, lower panel). (Scale bar: 10μm upper panel; 1.5μm lower panel)

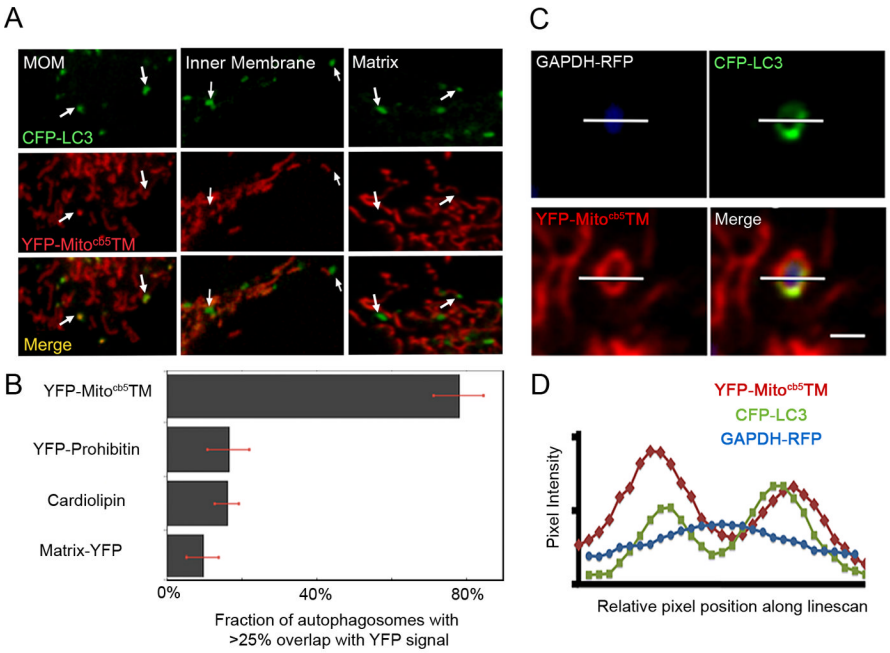

Figure 4. Assessing whether mitophagy underlies the appearance of YFP-Mito^{cb5}TM on autophagosomes

(A) Comparison of CFP-LC3 signal overlap with mitochondrial outer membrane (MOM), inner membrane and matrix signal. High-resolution imaging of NRK58B cells expressing MOM, inner membrane, and matrix markers revealed robust overlap of CFP-LC3 signal with the outer membrane, but not the inner membrane and matrix marker (see arrows). **(B)** Quantification of overlap of CFP-LC3 signal with mitochondrial markers. Quantification was done as described in Fig 3B. (**C**) Assessment of the association of YFP-Mito^{cb5}TM with the autophagosomal membrane. NRK58B cells were co-transfected with YFP-Mito^{cb5}TM and GAPDH-RFP, and starved. Signal from freely diffusing GAPDH-RFP was depleted by photobleaching to reveal CFP-LC3/YFP-Mito^{cb5}TM/GAPDH-RFP positive autophagosomes. High-resolution images of these structures revealed YFP-Mito^{cb5}TM present on the membrane, not trapped in the lumen. (Scale bar: 1.5μm) **(D)** Line-scan evaluation of CFP-LC3/YFP-Mito^{cb5}TM/GAPDH-RFP signal in autophagosomes. CFP-LC3 and YFP-Mitocb5TM pixel values along a transecting line (shown in A) exhibited two delineated peaks (membrane). In contrast GAPDH-RFP pixel values along this line exhibited a bell-curve like signal (lumen).

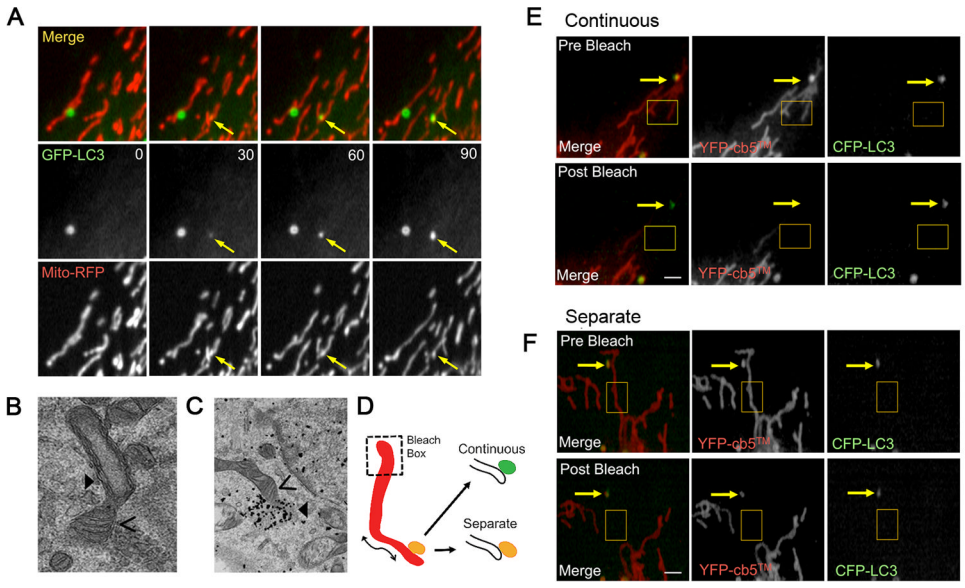

Figure 5. Assessing the association of starvation-induced autophagosomes and mitochondria

(A) Live-cell imaging of GFP-LC3 labeled autophagosomes and associated mitochondrial elements. NRK cells were transfected with the mitochondria matrix marker Mito-RFP and autophagosome marker GFP-LC3. High-resolution high speed imaging of starved cells showed autophagosomes grow during tight association with mitochondrial elements. See also supplementary Movie 4. **(B)** Electron microscopy of starved cells. Electron micrographs revealed the presence of multilammellar structures tightly associated with mitochondrial elements that exclude mitochondrial matrix. While rare in starved cells, these structures were never observed in unstarved cells. **(C)** Immuno EM of starved NRK58B cells labeled with gold-conjugated antibodies against CFP revealed clusters of gold particles that were observed tightly associated with proximal mitochondrial elements. **(D)** Model to demonstrate autophagosomal/mitochondrial membrane association assay. Photobleaching the distal end of a mitochondrial element depletes all YFP-Mito^{cb5}TM signal diffusing throughout the membrane. A YFP-Mito^{cb5}TM positive autophagosome whose membrane is continuous with the MOM also loses YFP-Mito^{cb5}TM signal via diffusion between the two associated organelles. A YFP-Mito^{cb5}TM positive autophagosome that is near but not continuous with the MOM retains YFP-Mito^{cb5}TM signal. **(E)** Data showing autophagosomal/mitochondrial membrane continuity. Autophagosomes that appeared to be associated with mitochondrial elements were identified. Distal ends of associated mitochondrial elements were targeted with 405nm and 490nm light (yellow box). Here, distal photobleaching depleted signal both from the mitochondria and the associated autophagosome outside the bleached region due to diffusion of the marker from outside the target region into the target region. (see loss of signal, bottom row, middle panel). (Scale bar: 2μm) **(F)** Autophagosomes that were spatially close but not associated retained signal after photobleaching of proximal mitochondrial elements (see retention of signal, bottom row, middle panel). (Scale bar: 2μm)

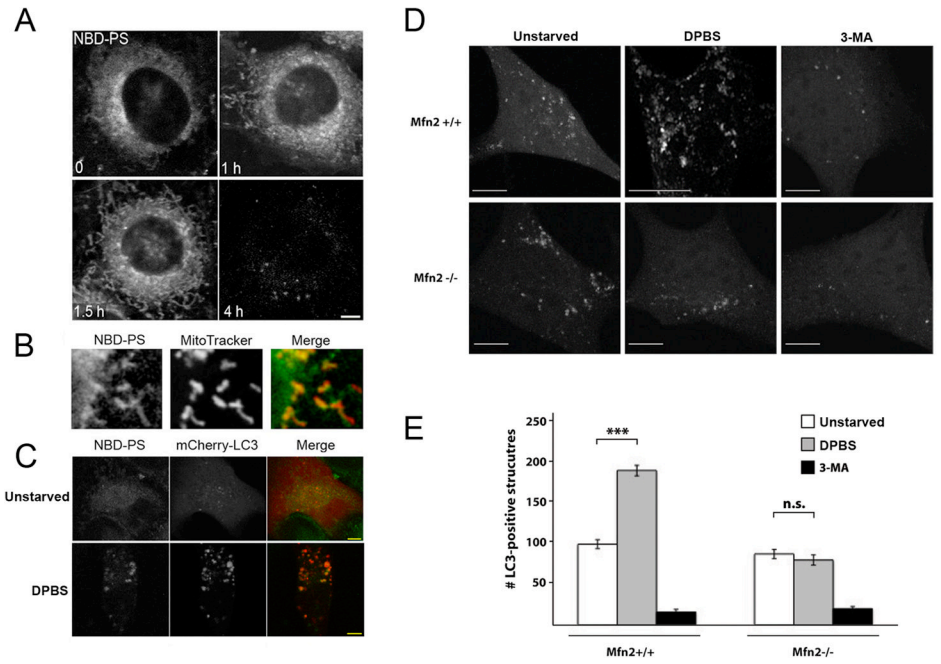

Figure 6. Mitochondrial lipid utilization in autophagosome formation

(A) Time course following loading of exogenous NBD-phosphatidylserine (NBD-PS). NRK cells were exposed to 220 μM NBD-PS, subsequently washed, and maintained in complete media. NBD signal rapidly accumulated in the mitochondria; by 4 hours, the majority of NBD signal was lost. (Scale bar: 5μm) **(B)** Colocalization of NBD-PS and mitochondria label. High-resolution imaging of Mitotracker red and NBD-PS revealed accumulation of NBD-PS signal in mitochondria one hour after exogenous NBD-PS loading. **(C)** NBD-labeling of starvation-induced autophagosomes. Cells were were labeled with NBD-PS and allowed 1 hour for NBD to accumulate in mitochondria before starvation. Upon starvation, the NBD-signal accumulated in induced (mCherry-LC3 positive) autophagosomes. (Scale bar: 5μM) **(D)** Disrupting ER-mitochondria connections by Mitofusin 2 deficiency. $Mfn2^{+/+}$ and $Mfn2^{-/-}$ MEF cells were transfected with human mCherry-LC3. $Mfn2^{+/+}$ and $Mfn2^{-/-}$ cells under nutrient rich starvation conditions show a similar degree of basal autophagy. Following starvation, $Mfn2^{-/-}$ cells fail to induce autophagy. $Mfn2^{+/+}$ cells show a dramatic increase in the number of autophagic structures, as well as depletion of the cytoplasmic and nuclear pools of mcherry-LC3 under starvation conditions. $Mfn2^{-/-}$ cells (like 3-MA treated cells) fail to induce more autophagosomes and clear cytosolic and nuclear mCherry-LC3. **(E)** Quantification of mCherry-LC3 positive structures in $Mfn2^{+/+}$ and $Mfn2^{-/-}$ cells. Autophagosomes were counted in 25 cells in three independent experiments.

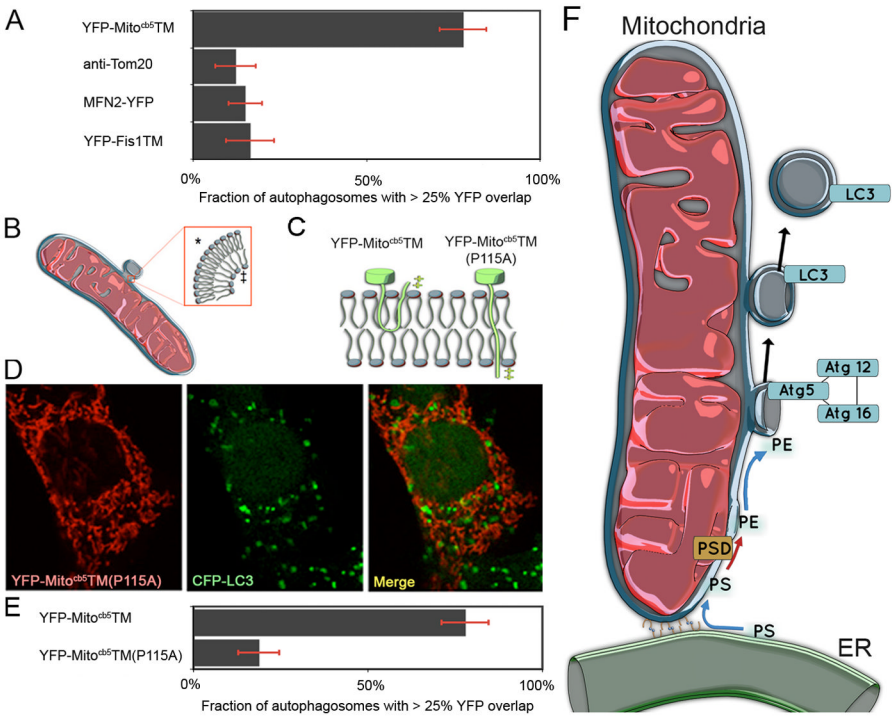

Figure 7. Maintenance of mitochondria during autophagosome biogenesis

(A) YFP-Mito^{cb5}TM uniquely labels autophagosomes; other outer membrane mitochondrial proteins with transmembrane domains that span the entire membrane fail to label autophagosomes. The paucity of other markers supports a unique mechanism for delivery of YFP-Mito^{cb5}TM marker due to its particular membrane association. **(B)** Schematic of proposed autophagosome bud site. Sharp membrane curvature selects for different lipids on the inner and outer leaflets of curved membranes. The distinct compositions of the leaflets can impede diffusion of proteins with preferences for particular lipid environments. **(C)** Schematic showing the reported forms of the cb5 transmembrane domain. The wild-type can exist in a kinked helix that interacts only with the outer leaflet of a target membrane. The P115A mutant intercalates across both leaflets of the bilayer. **(D)** Image showing lack of colocalization of the P115A cb5 mutant and the autophagosomal marker CFP-LC3. **(E)** Quantitative comparison of the two forms of the outer membrane marker. Mutating Proline115 to Alanine in the cb5^{TM} transmembrane domain abolishes its delivery to autophagosomes. (Scale bar in D: 10 μm). **(F)** Schematic for one proposed means by which autophagosomes might utilize mitochondrial membrane during autophagosome biogenesis (described in Discussion).